

# Phase Transitions in Higher Derivative Gravity

Tanay K. Dey<sup>1</sup>, Sudipta Mukherji<sup>2</sup>, Subir Mukhopadhyay<sup>3</sup> and  
Swarnendu Sarkar<sup>4</sup>

*Institute of Physics,  
Bhubaneswar 751 005, INDIA*

## ABSTRACT

This paper deals with black holes, bubbles and orbifolds in Gauss-Bonnet theory in five dimensional anti de Sitter space. In particular, we study stable, unstable and metastable phases of black holes from thermodynamical perspective. By comparing bubble and orbifold geometries, we analyse associated instabilities. Assuming AdS/CFT correspondence, we discuss the effects of this higher derivative bulk coupling on a specific matrix model near the critical points of the boundary gauge theory at finite temperature. Finally, we propose another phenomenological model on the boundary which mimics various phases of the bulk space-time.

September 2006

---

<sup>1</sup>e-mail: tanay@iopb.res.in

<sup>2</sup>e-mail: mukherji@iopb.res.in

<sup>3</sup>e-mail: subir@iopb.res.in

<sup>4</sup>e-mail: swarnen@iopb.res.in

# 1 Introduction

Black hole in AdS space has a remarkable property that it undergoes Hawking-Page (HP) phase transition [1]. Asymptotically AdS space allows two kinds of black hole configurations. By comparing their sizes with respect to the AdS scale, one can characterise these holes. While the small black holes have horizon sizes less than that of the AdS scale, the big black holes are larger than the AdS scale. These small black holes, however, are unstable with negative specific heat; leaving big black holes as the stable configurations in AdS space. Furthermore, it was noticed that, as we tune the temperature close to the inverse of the AdS scale, there is a first order phase transition. At a temperature below the inverse AdS scale, system prefers thermal AdS space, while at higher temperature, it is the big black hole phase which minimises the energy of the system. This crossover is known as HP transition. Via AdS/CFT correspondence [2], this phenomenon was found to have its imprint on the gauge theory residing on the boundary. Witten argued [3] that, on the boundary, the HP transition represents a large  $N$  deconfinement transition of the gauge theory at strong coupling.

Certain analytical continuation of the black hole metric in AdS space gives bubble of nothing solution [4, 5]. These are the analogues of Witten's Kaluza-Klein bubbles in flat space-time [6]. Bubble spacetime corresponds to time dependent configuration and, as we review later, in five dimensions, the boundary metric is  $dS_3 \times S^1$ . By using AdS/CFT correspondence, one then hopes to learn about gauge theory on time-dependent geometries. An important ingredient in the AdS/CFT correspondence is the principle of holography [7]. According to this principle, the physics of a gravitational theory is dual to a different theory in one lower dimension. Conversely, given a dual theory on a boundary, we must consider all possible bulk space-times whose boundaries have the same intrinsic geometry as the background of the dual theory. Now, given that the boundary metric is  $dS_3 \times S^1$ , there exists another bulk geometry known as AdS orbifold. These are the five dimensional analogues of BTZ black holes [8, 9]. These orbifolds are however unstable and below a critical size of the boundary  $S^1$ , they decay to bubbles of nothing [10, 11]. A bubble, once formed, expands exponentially and fills up the whole space-time. Though in AdS, this is similar to the of decay of the Kaluza-Klein space to nothing.

In this paper, after briefly reviewing the HP transition and orbifold decay in section 2, we analyse the response of these phenomena as we perturbatively increase the gravitational strength. Our study is partly motivated by recent works in [12–14].

In these papers, authors have argued in different ways that a version of HP transition occurs even at weak coupling gauge theory. By AdS/CFT dictionary, this would show up as a transition in strongly coupled gravity theory in the bulk. Noting the fact that string theory in AdS space is as yet poorly understood, we study a much simpler system in this paper. We add higher derivative terms in the supergravity action and study their effects on HP transition as well as on orbifold decay. We note here that higher derivative terms would arise in gravity action due to  $\alpha'$  corrections in underlying string theory. While a study with a general class of higher derivative terms would be desirable, in this work, we consider only the effects due to Gauss-Bonnet(GB) terms. One advantage of working with GB correction to the gravity action is that the black holes, bubbles and orbifolds can be constructed explicitly.

In section 3, we analyse the black holes in GB theory with a particular focus on their phase structures in five space-time dimensions. The phase structure depends crucially on the GB coupling. For certain range of coupling, there exists three black hole phases. We call them, small, intermediate or unstable and a big black hole phase. It turns out that there are two first order phase transitions. One of them is from small black hole to the big one at a temperature scale much lower than that of inverse AdS curvature. The other one is similar to that of usual HP transition where a crossover occurs from thermal AdS to the big black hole phase. We compute the change in HP temperature in powers of the GB coupling at the crossover.

In section 4, we study the bubbles in GB theory. We find that there exist bubble of nothing solutions for any value of the asymptotic circle. This is unlike the case in simple AdS gravity, where the bubble to exist, the circle size needs to be less than a critical value. Consequently, by computing energy densities of the bubble and orbifold spacetimes, we argue that orbifolds are always unstable and decay to bubble of nothing. The decay rate can then be easily computed by identifying the bounce solution.

Many papers in the recent past have analysed the partition function of free  $\mathcal{N} = 4$  super Yang-Mills theory and argued that the large  $N$  deconfinement transition occurs even at zero coupling [13, 14]. In fact, it turned out that the transition appears exactly at the Hagedorn temperature of the low temperature thermal AdS phase. Subsequently, non-perturbative  $1/N$  effects near the Hagedorn transition was studied in [15]. This has been analysed in the other limit of the 't Hooft coupling,  $\lambda \rightarrow \infty$  by proposing a phenomenological matrix model [16].

It is known that GB corrections arise in heterotic string theory, see for example [17]. In type IIB theory the corrections start off with  $R^4$ . In the case with Gauss

Bonnet terms we do not expect the boundary theory on  $S^3 \times S^1$  to be  $\mathcal{N} = 4$  Yang Mills theory. However in the limit  $\alpha' \rightarrow 0$  the boundary theory should reduce to the strongly coupled SYM theory. With the  $R^2$  corrections turned on, the gravity theory should correspond to some deformation of  $\mathcal{N} = 4$  SYM. In Section 5, we study this effective theory by using a phenomenological matrix model proposed in [16]. This model is characterised by two parameters which we call, following [16],  $a$  and  $b$ . Generally,  $(a, b)$  depend on the gauge theory temperature and the 't Hooft coupling  $\lambda$ . Following AdS/CFT, the effect of adding higher derivative terms in the bulk translates to  $\lambda$  corrections to the boundary gauge theory. *Assuming* an universal nature of the  $(a, b)$  model around the critical points, we analyse the  $\lambda$  dependence of parameters  $(a, b)$  around the HP points. We do this numerically in section 5.

Finally, in section 6, we construct a toy model which captures the whole phase diagram of the bulk. However, this requires introduction of four parameters in the matrix model potential. These four parameters again depend on the temperature as well as the gauge coupling. We then study the qualitative behaviour of this model. This paper ends with a discussion of our results. We hope to report on a similar analysis for the type IIB theory with  $R^4$  term in a future publication [18].

## 2 Black hole, bubble and AdS orbifold

In this section, we briefly recall black holes, bubbles and AdS orbifolds in AdS gravity in five dimensions. We review the instability associated with the AdS orbifolds and calculate the decay rate of these orbifolds to bubbles in the supergravity limit. Furthermore, we compute an enhancement of the decay rate due to string wrapping around a compact direction of the AdS orbifold. We also briefly review, following a suggestion due to Horowitz [19], as to how this decay may be catalysed by tachyon condensation in string theory.

### Black Hole:

Black hole in pure AdS-gravity is parametrised by a single parameter associated with the energy of the hole. Denoting this parameter as  $m$ , we may write the metric of the black hole as

$$ds^2 = -\left(1 + \frac{r^2}{l^2} - \frac{m}{r^2}\right) dt^2 + \left(1 + \frac{r^2}{l^2} - \frac{m}{r^2}\right)^{-1} dr^2 + r^2(d\theta^2 + \cos^2\theta d\Omega_2^2), \quad (1)$$

where  $l$  is related to the cosmological constant present in the action. This metric

asymptotically approaches AdS space. The singularity is at  $r = 0$  and the horizon is located at  $r_+$ , where  $r_+$  is a solution of equation

$$1 + \frac{r^2}{l^2} - \frac{m}{r^2} = 0. \quad (2)$$

The Euclidean version of the metric is free of any conical singularity if the Euclidean time has certain periodicity. Defining

$$r = r_+ + \left( \frac{r_+}{2l^2} + \frac{m}{2r_+^3} \right) \rho^2, \quad (3)$$

near  $r = r_+$ , we can write the metric as

$$ds^2 = d\rho^2 + \left( \frac{r_+}{l^2} + \frac{m}{r_+^3} \right)^2 \rho^2 d\chi^2 + r_+^2 d\Omega_3^2, \quad (4)$$

where, we have used  $t = i\chi$ . From here it follows that the metric is conically non-singular if  $\chi$  has a period

$$\Delta\chi = \frac{2\pi l^2 r_+^3}{r_+^4 + ml^2} = \frac{2\pi r_+ l^2}{2r_+^2 + l^2}. \quad (5)$$

Inverse of this periodicity is then identified with the black hole temperature. We note that, for a fixed temperature (above a certain critical value), we always get two black hole solutions with two different horizon sizes. We distinguish these two by calling them small and big black holes. At the critical temperature, both these black holes meet. It turns out that the smaller black hole is unstable with negative specific heat while the bigger one is stable. The free energy of the black holes is given by,

$$F = \frac{2\pi^2 r_+^2}{\kappa_5} \left( 1 - \frac{r_+^2}{l^2} \right). \quad (6)$$

Here,  $\kappa_5$  is related to the five dimensional gravitational constant. We note that if the size of the black hole is larger than the AdS scale  $l$ , the free energy becomes negative. Since this is less than the free energy of thermal AdS space, there is a first order phase transition. From (5), we see that for  $r_+ = l$ ,  $T = T_c = \frac{3}{2\pi l}$ . So the transition occurs from thermal AdS space phase to the black hole phase as we increase the temperature beyond  $T_c$ . The crossover between these two geometries is known as HP transition [1].

### Bubble:

The other space-time that is of our interest is the AdS bubble [4, 5, 10, 11]. The metric can be obtained by analytically continuing ( $t \rightarrow i\chi$  and  $\theta \rightarrow \pi/2 + i\tau$ ) the black hole solution given in (1). We get

$$ds^2 = \left( 1 + \frac{r^2}{l^2} - \frac{m}{r^2} \right) d\chi^2 + \left( 1 + \frac{r^2}{l^2} - \frac{m}{r^2} \right)^{-1} dr^2 + r^2 (-d\tau^2 + \cosh^2 \tau d\Omega_2^2). \quad (7)$$

If  $\chi$  is restricted to the period as in (5), the metric is non-singular for  $r \geq r_+$ . This geometry is known as a bubble of nothing solution. For large  $r$ , at any time  $\tau$ , the metric is  $\chi$  circle times a two sphere. This circle collapses at  $r = r_+$ . However, the two sphere approaches a finite size  $r_+^2 \cosh^2 \tau$ . This two sphere is the boundary of the bubble. We see that the metric is time dependent and is asymptotically  $dS^3 \times S^1$ . As can be seen from the dotted line in fig.6., below a certain critical value of  $\Delta\chi$ , for a given  $\Delta\chi$ , there are two possible bubble solutions. The smaller one, however, is expected to be unstable as its Euclidean continuation suffers from having modes with negative mass<sup>2</sup> [21]. The critical size of the  $\chi$  circle, above which there are no bubble solutions, is given by

$$\Delta\chi_c = \frac{l\pi}{\sqrt{2}} \quad \text{for } r_c = \frac{l}{\sqrt{2}}. \quad (8)$$

### AdS orbifold:

The AdS orbifold, that we consider here, has been discussed in great detail in [8,9,20]. A five dimensional AdS space is defined as the universal covering space of a surface which obeys

$$-x_0^2 + x_1^2 + x_2^2 + x_3^2 + x_4^2 - x_5^2 = -l^2, \quad (9)$$

where, as before,  $l$  is the AdS curvature radius. The orbifold is obtained by simply identifying points along the boost

$$\xi = \frac{r_+}{l}(x_4\partial_5 + x_5\partial_4), \quad (10)$$

where  $r_+$  being an arbitrary constant. Since the norm of the boost is given by  $\xi^2 = r_+^2(-x_4^2 + x_5^2)/l^2$ ,  $\xi^2$  can be positive or negative. However, to avoid closed time-like curves, the region  $\xi^2 < 0$  is removed from space-time. In an appropriate coordinate system this orbifolded space can be represented as

$$ds^2 = (\tilde{r}^2 - r_+^2)(-d\tilde{t}^2 + \frac{l^2}{r_+^2} \cosh^2(\frac{r_+\tilde{t}}{l})d\Omega_2^2) + \frac{l^2}{\tilde{r}^2 - r_+^2}d\tilde{r}^2 + \tilde{r}^2d\phi^2, \quad (11)$$

where  $r_+ \leq \tilde{r} \leq \infty$  and  $0 \leq \phi \leq 2\pi$ . Further defining

$$\tilde{r}^2 = r_+^2(1 + \frac{r^2}{l^2}), t = \frac{r_+\tilde{t}}{l}, \tilde{\chi} = r_+\phi, \quad (12)$$

the metric becomes,

$$ds^2 = (1 + \frac{r^2}{l^2})d\tilde{\chi}^2 + (1 + \frac{r^2}{l^2})^{-1}dr^2 + r^2[-dt^2 + \cosh^2 td\Omega_2^2]. \quad (13)$$

We should note here that, in these coordinates,  $0 < r < \infty$ . The Euclidean version of this space-time ( $t \rightarrow -i\theta - i\pi$ ) clearly resembles thermal AdS once we reinterpret the periodic coordinate  $\tilde{\chi}$  as Euclidean time. We record the metric here for later use:

$$ds^2 = \left(1 + \frac{r}{l^2}\right)d\tilde{\chi}^2 + \left(1 + \frac{r^2}{l^2}\right)^{-1}dr^2 + r^2[d\theta^2 + \cos^2\theta d\Omega_2^2]. \quad (14)$$

### Instabilities and decay rates:

We now see from (13) and (7) that both these space-times have the same asymptotic geometry. The boundary is time dependent and is given by  $dS^3 \times S^1$ . However, a notable difference is while the orbifold exists for any size of the asymptotic  $S^1$ , the bubble appears only when this boundary circle has a maximum critical size. The size is given by the expression in (8). Boundary energy densities of the orbifold and the bubble are computed in [5]. They are given by

$$\rho_{\text{orbi}} = -\frac{1}{64\pi Gl}, \quad \rho_{\text{bubble}} = -\frac{1}{16\pi Gl^3}\left(m + \frac{l^2}{4}\right). \quad (15)$$

Let us now consider the case where the size of the boundary circle is less than the critical value given in (8). In the bulk, we can have both the bubble or the orbifold geometry. However, in view of equation (15), we see that the orbifold will decay to the bubble of nothing by radiating away its energy [10, 11]. This is the analogue of Witten's decay of Kaluza-Klein vacuum to a bubble of nothing [6]<sup>5</sup>.

As in the case of Kaluza-Klein decay, it is possible to find the bounce solution which mediates this decay. This was discussed in some detail in [11]. As analysed there, it is the Euclidean continuation of the smaller Schwarzschild black hole which acts as a bounce. The metric for the bounce is therefore

$$ds^2 = \left(1 + \frac{r^2}{l^2} - \frac{m}{r^2}\right)d\chi^2 + \left(1 + \frac{r^2}{l^2} - \frac{m}{l^2}\right)^{-1}dr^2 + r^2(d\theta^2 + \cos^2\theta d\Omega_2^2). \quad (16)$$

Having identified the bounce, we can calculate the semiclassical decay rate from the orbifold to the bubble by evaluating the action difference between Euclideanised orbifold (14) and the bounce (16). Though individual actions diverge due to large volume, the difference remains finite once we require same asymptotic boundary conditions for  $\tilde{\chi}$  in (14) and for  $\chi$  in (16). This is obtained by setting

$$\sqrt{1 + \frac{R^2}{l^2}}\beta_{\tilde{\chi}} = \sqrt{1 + \frac{R^2}{l^2} - \frac{m}{R^2}}\beta_{\chi}. \quad (17)$$

---

<sup>5</sup>When embedded in supersymmetric theory, one employs antiperiodic boundary condition of the fermions around the circle. This breaks supersymmetry completely

Here  $\beta_{\tilde{\chi}}$  is the period of  $\tilde{\chi}$  in (14) and  $\beta_{\chi}$  is the period of  $\chi$  in (16); the expression of the later is given in (5). Now the difference in actions is given by

$$\begin{aligned}
\Delta I &= I_{\text{bounce}} - I_{\text{orbifold}} \\
&= \frac{2 \times 4}{16\pi G l^2} \left[ \int_0^{\beta_{\chi}} d\chi \int_{r_+}^R r^3 dr \int d\Omega_3^2 - \int_0^{\beta_{\tilde{\chi}}} d\tilde{\chi} \int_0^R r^3 dr \int d\Omega_3^2 \right] \\
&= \frac{\omega_3}{8G} \left( \frac{r_+^3 l^2 - r_+^5}{2r_+^2 + l^2} \right). \tag{18}
\end{aligned}$$

Here  $\omega_3$  is the volume of unit three sphere. In getting the last expression we have made use of the boundary condition (17).

### Enhancement of decay rate due to string wrapping the circle:

On generic grounds, we expect an enhancement of orbifold decay rate when a Nambu-Goto string wraps around the circle  $\tilde{\chi}$ . This is what we intend to compute in this subsection. We noted that the decay of the orbifold requires a bounce solution with a negative mode in its spectrum of small fluctuation. The small Euclidean AdS-Schwarzschild black hole that we analysed in the previous section has such a mode [21]. In what follows, we will assume that the presence of a string does not remove this non-conformal negative mode. With this assumption, it is now easy to see how the decay rate changes as we wrap a string with action

$$S = T \int d^2\xi \sqrt{\det\gamma} \tag{19}$$

along  $\tilde{\chi}$  direction of the orbifold and  $\chi$  direction of the bounce solution. Here,  $\gamma$  is the induced metric on the string. We expect that the change in the decay rate will be proportional to the exponential of the action difference  $\Delta S = S_{\text{bounce}} - S_{\text{orbifold}}$ . This quantity can be easily computed as follows:

$$\begin{aligned}
\Delta S &= S_{\text{bounce}} - S_{\text{orbifold}} \\
&= T \int d^2\xi \sqrt{\det\gamma_{\text{bubble}}} - T \int d^2\xi \sqrt{\det\gamma_{\text{orbifold}}} \\
&= T \int_0^{\beta_{\chi}} d\tau \int_{r_+}^R dr - T \int_0^{\beta_{\tilde{\chi}}} \int_0^R dr \\
&= T \frac{2\pi l^2 r_+^2}{2r_+^2 + l^2}. \tag{20}
\end{aligned}$$

To get to the last step, we have used (17) and also made a large  $R$  approximation<sup>6</sup>. From the above expression we see that the decay rate increases with  $r_+$ . This, in turn, implies that enhancement is larger for larger size bubble in the final state. We see from the above expression that  $\Delta S$  increases with string tension  $T$ . However, for a string with large energy density, we would have to go beyond test string approximation.

### Decay via tachyon:

In a recent paper [19], Horowitz has argued that a black string can catalyse Witten's decay process. When a black brane is wrapped around a compact circle, the circle size becomes a function of the position. For a suitable choice of brane, regardless of its asymptotic size, this circle can reach string scale at the brane horizon. In fact, tuning the charges of the branes, this circle size can be made to vary very slowly. For an anti-periodic boundary condition of the fermions around this circle, one expects a tachyonic mode to appear as the size shrinks to string scale. This mode may then induce a topology changing process by pinching off the circle at the horizon. This, in turn, creates a bubble. A concrete example of this is the  $D3$  brane in ten dimension. For our purpose, instead of a flat space-time, let us consider  $N$   $D3$  branes filling up the boost orbifold  $R^{1,1}/Z$ . In the near horizon limit one gets AdS orbifold in five dimensions [11]. On the other hand, after the tachyon condensation, we have a bubble of the kind that we have been considering. Since this decay is catalysed by a string scale process, one would expect the rate to be much faster than the one through supergravity bounce.

In the next section we discuss black holes, bubbles and orbifolds in GB theory. We study how the above features change as a function of the GB coupling.

## 3 Gauss-Bonnet black holes

We start by considering  $(n + 1)$  dimensional gravitational action in the presence of a negative cosmological constant  $\Lambda$  along with a GB term.

$$I = \int d^{n+1}x \sqrt{-g_{n+1}} \left[ \frac{R}{\kappa_{n+1}} - 2\Lambda + \alpha(R^2 - 4R_{ab}R^{ab} + R_{abcd}R^{abcd}) \right]. \quad (21)$$

This action possesses black hole solutions which we call GB black holes [17, 23–27]. In the above action,  $\alpha$  is the GB coupling. As the higher derivative corrections are expected to appear from the  $\alpha'$  corrections in underlying string theory, we will often

---

<sup>6</sup> A similar computation was performed in [22] in the context of Witten's bubble

refer to such corrections as  $\alpha'$  corrections in this paper. The metric of these holes can be expressed as

$$ds^2 = -V(r)dt^2 + \frac{dr^2}{V(r)} + r^2 d\Omega_{n-1}^2, \quad (22)$$

where  $V(r)$  is given by

$$V(r) = 1 + \frac{r^2}{2\hat{\alpha}} - \frac{r^2}{2\hat{\alpha}} \left[ 1 - \frac{4\hat{\alpha}}{l^2} + \frac{4\hat{\alpha}m}{r^n} \right]^{\frac{1}{2}}. \quad (23)$$

We first define various parameters that appear in the above equation.  $d\Omega_{n-1}^2$  is the metric of a  $n - 1$  dimensional sphere.  $l^2$  is related to the cosmological constant as  $l^2 = -n(n - 1)/(2\kappa_{n+1}\Lambda)$ . Furthermore, we have defined  $\hat{\alpha} = (n - 2)(n - 3)\alpha\kappa_{n+1}$ , where  $\kappa_{n+1}$  is the  $n + 1$  dimensional gravitational constant. The parameter  $m$  in (23) is related to the energy of the configuration as

$$M = \frac{(n - 1)\omega_{n-1}m}{\kappa_{n+1}}, \quad (24)$$

where  $\omega_{n-1}$  is the volume of the  $n - 1$  dimensional unit sphere. Asymptotically, the metric (23) goes to AdS space, since in this limit

$$V(r) = 1 + \left[ \frac{1}{2\hat{\alpha}} - \frac{1}{2\hat{\alpha}} \left( 1 - \frac{4\hat{\alpha}}{l^2} \right)^{\frac{1}{2}} \right] r^2. \quad (25)$$

We see from here that the metric is real if and only if

$$\hat{\alpha} \leq l^2/4. \quad (26)$$

In our discussion, we will always consider  $\hat{\alpha}$  satisfying the above bound. The metric (22) has a central singularity at  $r = 0$ . The zeros of  $V(r)$  correspond to the locations of the horizons.

In five dimension, for which  $n = 4$ , there is a single horizon at

$$r^2 = r_+^2 = \frac{l^2}{2} \left[ -1 + \sqrt{1 + \frac{4(m - \hat{\alpha})}{l^2}} \right]. \quad (27)$$

We note here that for a black hole to exist  $m > \hat{\alpha}$ .

Thermodynamics of these black holes can be obtained via standard Euclidean action calculation. Such calculations were performed, for example, in [26]. Following these computations, the free energy and temperature can be written down as

$$F = \frac{\omega_{n-1}r_+^{n-4}}{\kappa_{n+1}(n-3)(r_+^2 + 2\hat{\alpha})} \left[ (n-3)r_+^4 \left( 1 - \frac{r_+^2}{l^2} \right) - \frac{6(n-1)\hat{\alpha}r_+^4}{l^2} + (n-7)\hat{\alpha}r_+^2 + 2(n-1)\hat{\alpha}^2 \right], \quad (28)$$

$$T = \frac{(n-2)}{4\pi r_+(r_+^2 + 2\hat{\alpha})} \left[ r_+^2 + \frac{n-4}{n-2}\hat{\alpha} + \frac{n}{n-2} \frac{r_+^4}{l^2} \right]. \quad (29)$$

The black hole entropy is given by

$$S = \int T^{-1} \left( \frac{\partial M}{\partial r_+} \right) dr_+ = \frac{4\pi\omega_{n-1}r_+^{n-1}}{\kappa_{n+1}} \left[ 1 + \frac{n-1}{n-3} \frac{2\hat{\alpha}}{r_+^2} \right], \quad (30)$$

and the specific heat is

$$C = \frac{\partial M}{\partial T} = \frac{4\pi(n-1)\omega_{n-1}r_+^{n-3}(r_+^2 + 2\hat{\alpha})^2 [\hat{\alpha}l^2(n-4) + r_+^2(l^2(n-2) + nr_+^2)]}{\kappa_{n+1} [\hat{\alpha}r_+^2(6nr_+^2 - l^2(n-8)) + r_+^4(nr_+^2 - (n-2)l^2) - 2(n-4)\hat{\alpha}^2l^2]}. \quad (31)$$

Many interesting features of the GB black holes, related to local and global stabilities, can be inferred from a detailed study of the thermodynamic quantities. In the rest of the section, we proceed to do so by considering the holes in five dimensions ( $n = 4$ ). Let us first introduce two dimensionless quantities

$$\bar{\alpha} = \frac{\hat{\alpha}}{l^2}, \text{ and } \bar{r} = \frac{r_+}{l}. \quad (32)$$

We would like to express various thermodynamic quantities in terms of these dimensionless constants. The free energy given in (29) can be written as

$$F = -\frac{\omega_3 l^2}{\kappa_5 (\bar{r}^2 + 2\bar{\alpha})} \left[ \bar{r}^6 + (18\bar{\alpha} - 1)\bar{r}^4 + 3\bar{\alpha}\bar{r}^2 - 6\bar{\alpha}^2 \right]. \quad (33)$$

It then follows from (33), that within the range of allowed value of the coupling  $\bar{\alpha}$  (see (26)),  $F$  starts being positive at  $\bar{r} = 0$  and changes sign only once as we increase  $\bar{r}$ . The number of extrema of the free energy, however, crucially depends on  $\bar{\alpha}$ . In particular, when  $\bar{\alpha}$  is in the region

$$0 < \bar{\alpha} \leq \frac{1}{36}, \quad (34)$$

$F$  has three extrema. At these points,  $F$  takes non-zero positive values. However, for

$$\frac{1}{36} \leq \bar{\alpha} \leq \frac{1}{4}, \quad (35)$$

$F$  has no extremum for any non-zero  $\bar{r}$ . It starts with a nonzero value at  $\bar{r} = 0$ , then decreases monotonically and becomes negative at large  $\bar{r}$ . Typical behaviour of the free energy as a function of  $\bar{r}$  is shown fig.1. We will refer back to this plot when we analyse the stability of these holes.

For now, we turn our attention to the temperature of the black holes. It follows from (29) that the temperature is given by

$$T = \frac{\bar{r} + 2\bar{r}^3}{2\pi l(\bar{r}^2 + 2\bar{\alpha})}. \quad (36)$$

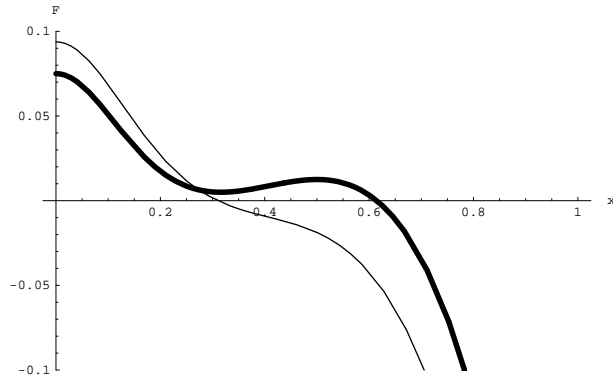


Figure 1: Free energy as a function of  $x = \bar{r}$  for different values of  $\bar{\alpha}$ . The thicker line is for  $\bar{\alpha} = 1/40$  and the other one  $\bar{\alpha} = 1/32$ .

At  $\bar{r} = 0$ , temperature starts out from zero and, regardless of the value of  $\bar{\alpha}$ , it increases for small  $\bar{r}$ . However, at larger  $\bar{r}$ , the number of extrema depends on  $\bar{\alpha}$ . In the region given in (34), there are two of these extrema. Both of these disappear as we increase  $\bar{\alpha}$  to region (35). A plot of the temperature as a function of  $\bar{r}$  is shown in fig.2.

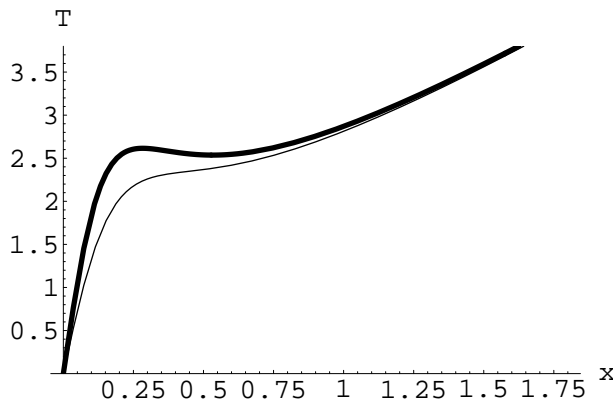


Figure 2: Temperature as a function of  $x = \bar{r}$  for different values of  $\bar{\alpha}$ . The thicker line is for  $\bar{\alpha} = 1/44$  and the other one  $\bar{\alpha} = 1/30$ .

To examine the phase structure of these black holes, it is instructive to consider the behaviour of the free energy as a function of temperature (for different values of  $\bar{\alpha}$ ). From (33) and (36), it is possible to construct the temperature dependence of the free energy. However, the analytical expression is not very illuminating. Therefore, we plot the nature of the free energy as a function of temperature in fig.3. This plot is for two different values of  $\bar{\alpha}$  belonging to the two different regions given in (34) and (35). Note that, as we increase  $\bar{\alpha}$  from region (34) to region (35), nature of  $F$  changes

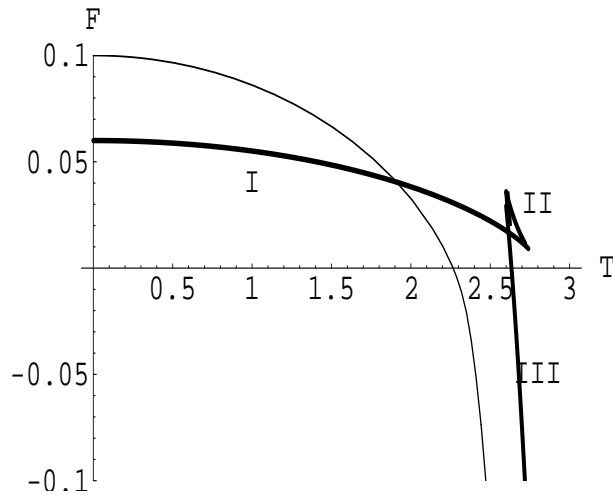


Figure 3: Free energy as a function of temperature. The thicker one is for  $\bar{\alpha} = 1/50$  while the other one is for  $\bar{\alpha} = 1/30$ .

at a critical value  $\bar{\alpha} = \bar{\alpha}_c = 1/36$ . We therefore study these two regions separately.

#### Phase structure for $\bar{\alpha} \leq \bar{\alpha}_c$ :

When  $\bar{\alpha} \leq \bar{\alpha}_c$ , the free energy is shown by the thicker line in fig.3. At low temperature, it has only one branch (shown as branch I in the figure). However, when the temperature is increased beyond a certain value (which we call  $T_1$ ), two new branches appear (II and III). One of these two branches (II) meets branch I at a temperature beyond, say  $T_1$ , and they both disappear. On the other hand, branch III continues to decrease rapidly, cuts branch I at temperature, say  $T_2$ , and becomes negative at a temperature which we will call  $T_c$  in the future. While computing specific heat using (31), we find that it is positive for branch I, and III. Therefore, these phases correspond to stable black holes. They, however, differ in their sizes; branch I represents smaller sized black holes than that of branch III. Going back now to branch II, we find that the specific heat is negative. We, therefore, conclude that branch II represents an unstable phase of the black hole.

The above picture is similar to that of the van der Waals gas. In particular, the Gibbs free energy of van der Waals gas, for an isotherm, behaves in a similar manner as we vary pressure. A thermodynamic equilibrium state is reached by minimising the Gibbs free energy. Likewise, in our case, equilibrium state would correspond to branch I of the free energy all the way up to temperature  $T_2$  and then branch III from temperature  $T_2$  and above. The free energy curve then remains concave as expected for a thermodynamical system. We, however, note that since there is a discontinuity

of  $dF/dT$  at  $T = T_2$ , one has a first order phase transition at  $T_2$ . Two black hole phases would differ from each other at this point by a discontinuous change in their entropies. We will call these as the first Hawking-Page (HP1) transition for reasons that will be obvious later.

This phase structure can be nicely described by constructing a Landau function around the critical point. By identifying the dimensionless quantity  $\bar{r}$  as an order parameter, we can construct a function  $\Phi(T, \bar{r})$  as<sup>7</sup>

$$\Phi(T, \bar{r}) = \frac{\omega_3 l^2}{\kappa_5} (3\bar{r}^4 - 4\pi l T \bar{r}^3 + 3\bar{r}^2 - 24\pi \bar{\alpha} l T \bar{r} + 3\bar{\alpha}). \quad (37)$$

At the saddle point of this function, that is when  $\frac{\partial \Phi}{\partial \bar{r}} = 0$ , we get back the expression of the temperature given in (36). If we then substitute back the expression of temperature in to (37),  $\Phi(\bar{r})$  reduces to the free energy given in (33). As can be seen from fig.4., for temperature  $T < T_2$ ,  $\Phi(T, \bar{r})$  has only one global minimum. This corresponds to the small black hole phase. However, at  $T = T_2$ , appearance of two degenerate minima suggests a coexistence of small and big black hole phases. Finally for temperature beyond  $T_2$ , only the big black holes phase remains (as this phase minimizes the Landau function). Clearly, there is a discrete change in the order parameter  $\bar{r}$  at  $T = T_2$ . This is what we expect for a first order phase transition.

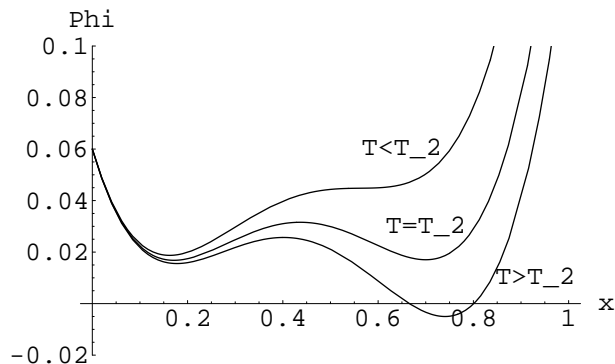


Figure 4: Landau function  $\Phi$  as a function of order parameter  $x = \bar{r}$  for different temperatures. We have taken  $\bar{\alpha} = 1/50$ .

### Phase structure for $\bar{\alpha} > \bar{\alpha}_c$ :

For  $\bar{\alpha} > \bar{\alpha}_c$ , the free energy curve is shown by the thin line in fig.3. Unlike the previous case, free energy and its derivatives do not show any discontinuity. Therefore,

<sup>7</sup>To construct the Landau function, we employ a method similar to the one discussed in [28, 29].

there is no HP1 transition. Only a single black hole phase is found to exist at any temperature.

### Global phase structure of GB black holes:

As discussed earlier, for black holes with  $\bar{\alpha} = 0$ , there is a crossover from AdS to AdS black holes at a critical temperature  $\frac{3}{2\pi l}$ . What happens to this transition as we turn on  $\bar{\alpha}$ ? In this situation, we note that we still have two geometries to consider. First one is again a thermal AdS with metric being the Euclidean continuation of (22). The function  $V(r)$  is given in (25). We identify this thermal AdS space, with  $\bar{\alpha}$  dependent effective cosmological constant, has zero free energy. However, we see from fig.3. that above a critical temperature, the free energy of the GB black hole becomes negative, making it more stable compared to the effective AdS geometry. We identify this as a HP2 point. This crossover temperature can be computed as a power series in  $\bar{\alpha}$  and is given by

$$T_c = \frac{3}{2\pi l} - \frac{33\bar{\alpha}}{4\pi l} + \mathcal{O}(\bar{\alpha}^2). \quad (38)$$

We notice here that the GB correction reduces the transition temperature. Similar phenomenon was noticed earlier in many AdS-gravity theories with higher curvature terms [30–33]. The global phase structure is shown in fig.5.

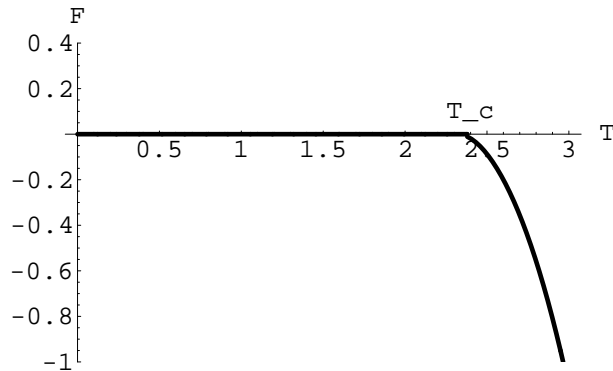


Figure 5: Global phase structure of GB black holes. For temperature  $T < T_c$ , AdS lowers the free energy, on the other hand for  $T > T_c$  the black hole phase is preferred. This plot is for  $\bar{\alpha} = 1/30$ .

To this end, we would like to point out that the above picture of GB black holes is quite similar to that of the five dimensional charged AdS black holes [34, 35]. The stability properties of the charge black holes depend on whether we are considering

fixed potential ensemble or fixed charge ensemble. For the case of fixed charge ensemble, various phases of black holes resemble that of the thick line in fig.3. As in our case, small black holes and large black holes are separated by a first order phase transition point. However, a major difference is that for the charged black holes, in fixed charge ensemble, thermal AdS is not a solution. Consequently, these holes are globally stable. This is unlike GB black holes, where there is a HP2 transition. Below HP2 temperature, they are unstable.

## 4 Bubbles in GB theory and instabilities

In this section, we turn our attention to bubble spacetime in GB theory. After constructing these bubbles, we compute their energy densities. We find that due to the presence of these bubbles with same asymptotic structure as of the AdS orbifolds in GB theory, the orbifolds become unstable. The nature of these decays depend on the value of  $\bar{\alpha}$ . In what follows, we will be mainly interested in studying these instabilities as a function of  $\bar{\alpha}$ . We will also highlight the differences that occur when we compare the present situation with the one with  $\bar{\alpha} = 0$ .

The bubbles in the GB theory can be constructed by analytically continuing the coordinates of the GB black holes as  $t \rightarrow i\chi, \theta \rightarrow \pi/2 + i\tau$ . Here theta parametrises one of the angles of  $d\Omega_{n-1}$  in (22). The solutions then takes the form

$$ds^2 = V(r)d\chi^2 + \frac{dr^2}{V(r)} - r^2d\tau^2 + r^2\cosh^2\tau d\Omega_{n-3}^2, \quad (39)$$

where  $V(r)$  is given in (23). Above metric is nonsingular in the region  $r \geq r_+$  if  $\chi$  has a periodicity

$$\Delta\chi = \frac{4\pi\bar{r}l(\bar{r}^2 + 2\bar{\alpha})}{(n-2)(\bar{r}^2 + \frac{n-4}{n-2}\bar{\alpha} + \frac{n}{n-2}\frac{\bar{r}^4}{l^2})}. \quad (40)$$

In the following we will use dimensionless quantity  $\Delta\bar{\chi} = \Delta\chi/l$  to parametrise the circle. We first note that at asymptotically large distance, the metric reduces to  $dS_{n-1} \times S^1$  where  $S^1$  corresponds to the  $\chi$  circle. More precisely, up to a conformal scaling by  $L^2/r^2$ , the boundary metric becomes

$$ds^2 = d\chi^2 + L^2(-d\tau^2 + \cosh^2\tau d\Omega_{n-2}^2). \quad (41)$$

In the above equation, we have defined

$$L = \sqrt{2\hat{\alpha}} \left[ 1 - \left( 1 - \frac{4\hat{\alpha}}{l^2} \right)^{\frac{1}{2}} \right]^{-\frac{1}{2}}. \quad (42)$$

At  $r = r_+$ , the proper radius of this circle collapses at  $V(r) = 0$ . However, the  $n - 2$  sphere approaches a finite size  $r_+^2 \cosh^2 \tau$ . Therefore (39) represents a bubble of nothing in GB theory with size  $r_+$ . In the rest of this section, we will mostly focus ourselves on the bubbles in five dimensions.

Many of the features of these bubbles can be understood from the behaviour of the periodicity  $\Delta\bar{\chi}$  as a function of  $\bar{\alpha}$  and  $\bar{r}$ . Firstly, as can be seen from fig.6., for any non-zero  $\bar{\alpha}$ , there exists a bubble for any size of the  $\chi$  circle. This is very much unlike the case when  $\bar{\alpha} = 0$  where there is a critical radius above which the bubbles are no longer present. Secondly, for a given  $\bar{\alpha}$  in the range (34), and for a given periodicity of  $\chi$ , there can be at most three bubbles of varied sizes. This can be seen from the solid line in fig.6. However, as we increase  $\bar{\alpha}$  above  $1/36$  and go to the range (35), for fixed  $\Delta\chi$ , we get a single bubble of fixed size. This is shown by the dashed line in fig.6.

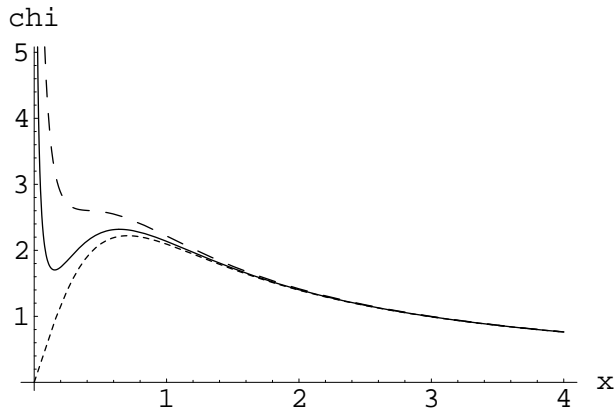


Figure 6: Plot of  $\Delta\bar{\chi}$  as a function  $x = \bar{r}$ . The dashed line is for  $\bar{\alpha} = 1/34$ . The solid line is for  $\bar{\alpha} = 1/50$  and the dotted line is for  $\bar{\alpha} = 0$ .

Continuing our discussions in five dimensions, let us note that as in the case of AdS gravity, in GB theory, we also have another geometry with the same asymptotic metric. These are the AdS orbifolds (13) with the AdS curvature  $l$  replaced by  $L$  as in (42).

The asymptotic boundary of the GB bubble spacetime is  $dS_3 \times S^1$ . One would then expect, by AdS/CFT correspondence, that some deformation of  $\mathcal{N} = 4$  SU(N) Yang-Mills theory at large but *finite*  $\lambda$  should be dual to the bubble. Clearly, similar to the AdS bubbles, for the GB bubbles, the CFT lives on a time dependent space. The boundary stress tensor can be computed from the bulk stress tensor. These bulk

stress tensor components, for GB bubbles, can easily be obtained and are given by

$$\begin{aligned}
T_\tau^\tau &= \frac{1}{\kappa_5 L^3} m, \\
T_\chi^\chi &= -\frac{3}{\kappa_5 L^3} m, \\
T_\theta^\theta &= \frac{1}{\kappa_5 L^3} m, \\
T_\phi^\phi &= \frac{1}{\kappa_5 L^3} m,
\end{aligned} \tag{43}$$

where we have parametrised  $d\Omega_2$  by the coordinates  $\theta$  and  $\phi$ . We note here that the components of the stress-tensor computed with respect to the orbifold in GB theory<sup>8</sup>. Positive sign of  $T_\tau^\tau$  implies that the solution has negative mass.

As of now, we have learned that, in GB theory, bubble space exists for any value of  $m$ . This, in turn, means that we can have a bubble of any size. Furthermore, we note that the bubble and AdS orbifold have asymptotically the same metric, namely  $dS_3 \times S^1$ . The energy density of the bubble spacetime is however less than that of the orbifold. We may, therefore, conclude that AdS orbifold is an *unstable* background in GB theory. It will always decay to bubble by radiating away its energy. As a result, bubble of any size will be produced. Once it is produced, due to the time-dependent nature of the metric, the radius of the bubble will increase exponentially with time.

It is easy to compute the decay rate from the orbifold to bubble. This can be done, as before, by identifying the bounce solution.

## 5 Matrix Model : Some numerical computation

In the previous sections we have analysed the phase structure of the gravitational theory in the presence of a higher derivative correction. In the light of the AdS/CFT correspondence we would now like to analyse these phases from the gauge theory on the boundary. Specifically, we will study the thermal aspects of the  $SU(N)$  gauge theory on the boundary of  $AdS_5$  which is  $S^3 \times S^1$ . The effective theory on the boundary can be described by an unitary matrix model:

$$Z(\lambda, T) = \int dU e^{S_{eff}(U)}, \tag{44}$$

---

<sup>8</sup>One easy way to compute these expressions is to first calculate various components of stress-energy tensor for GB black holes. The formalism to compute  $T_{\mu\nu}$  for the GB black holes is given in [36]. One can then make a proper analytical continuation to get stress tensor for the GB bubbles.

where  $U = P \exp(i \int_0^\beta A(\tau) d\tau)$  and  $A(\tau)$  is the zero mode of  $A_0$  on  $S^3$ . This is the lightest mode, and the effective action is obtained by integrating out all the massive modes. In general  $S_{eff}(U)$  is a polynomial in the traces of  $U$  and its powers that are allowed by the  $Z_N$  symmetry. The coefficients of these terms depend on the 'tHooft coupling  $\lambda$  (that is related to  $\alpha'$  by,  $\alpha' \sqrt{2\lambda} = l^2$  from the AdS/CFT correspondence) and temperature  $T$ .

These coefficients have been worked out in the weak coupling expansion in [37]. In our analysis we will restrict ourselves to the first two terms,

$$S_{eff}(U) = a \text{tr} U \text{tr} U^\dagger + \frac{b}{N^2} (\text{tr} U \text{tr} U^\dagger)^2, \quad (45)$$

where,  $a$  and  $b$  are functions of temperature  $T$  and  $\lambda$ . An order parameter characterising the deconfined phase of the gauge theory is given by the expectation value of the Polyakov loop  $1/N \langle \text{tr} U \rangle$ .

The saddle point equations for this effective theory are given by,

$$\begin{aligned} a\rho + 2b\rho^3 &= \rho & 0 \leq \rho \leq \frac{1}{2} \\ &= \frac{1}{4(1-\rho)} & \frac{1}{2} \leq \rho \leq 1, \end{aligned} \quad (46)$$

where  $\rho^2 = (1/N^2) \text{tr} U \text{tr} U^\dagger$ . As mentioned this matrix model contains only the first two terms of the effective gauge theory in the weak coupling expansion. It was shown in [16] that with this truncation, in the large  $N$  limit one can reproduce the same thermodynamic features as of the bulk black hole thermodynamics near the critical points. This model thus appears to fall in the same universality class as that of the boundary effective gauge theory in the strong coupling limit.

The phase structure in the bulk theory that we have discussed in Section 3 contains various distinct qualitative features depending on the value of the correction parameter  $\alpha'$ . For nonzero  $\alpha'$ , the phase diagram is modified in the regime where  $r$  is small compared to  $\sqrt{\alpha'}$ . However as long as  $r_+$  (the solutions corresponding to the black holes at a particular temperature) are greater than  $\alpha'$ , the phase diagram is qualitatively the same as that of the bulk theory without higher derivative corrections. In this domain, it makes sense to compare the bulk physics with that of the boundary  $(a, b)$  matrix model discussed in the earlier paragraph. In the next section we will propose a matrix model potential that captures the bulk physics including the solution  $r_+$  which is less than  $\sqrt{\alpha'}$ .

The following part of this section is devoted to the study of this matrix model numerically, incorporating the corrections due to the finite 'tHooft coupling  $\lambda$ . In

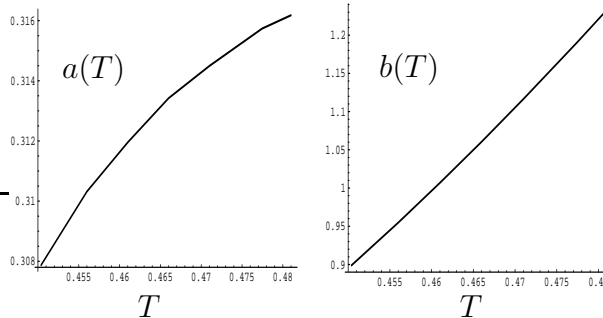


Figure 7: Plots of  $a(T, 0)$  and  $b(T, 0)$

this analysis we will take  $N \rightarrow \infty$ . We first work in the limit  $\lambda \rightarrow \infty$  and then by taking  $\lambda$  large but finite. The main aim is to compute  $a$  and  $b$  as functions of  $T$  and of  $\lambda$  (to the first order in  $1/\sqrt{\lambda}$ ). This will be done by comparing the matrix model potential with the action on the gravity side with  $\alpha'$  corrections. In this paper we are considering the corrections due to the Gauss-Bonnet term. As mentioned before  $R^2$  corrections are not known to occur in the supergravity limit of type IIB theory. However the following analysis is a fruitful exercise that can easily be adapted for the  $R^4$  terms that arise in this theory.

The comparison between matrix model potential and the action of the bulk theory is valid as long as we can neglect the string loop corrections. The corresponding temperature at which the supergravity description breaks down is identified as the Gross-Witten transition point in [16, 39] on the matrix model side.

Let  $T_0$  be the temperature at which the black hole nucleation starts. For  $T > T_0$ , it is well known that for the gravity theory without  $\alpha'$  corrections, one gets two solutions for the black hole. The small black hole is unstable and the larger one stable. The larger one undergoes a Hawking-Page transition at  $T = T_c$ . It was shown by Witten [3] that thermal  $AdS_5$  corresponds to the deconfined phase of the large  $N$  gauge theory on the boundary. A natural order parameter that characterises the deconfined phase is the Polyakov loop. In this matrix model it is  $\rho$ .

Let us study the case without  $\alpha'$  corrections first. This corresponds to the  $\lambda \rightarrow \infty$  limit. Consider  $T > T_0$ , for which we have<sup>9</sup>

$$2a\rho_{1,2}^2 + 2b\rho_{1,2}^4 + \log(1 - \rho_{1,2}) + f = -I_{1,2}, \quad (47)$$

<sup>9</sup>We will set  $l, \omega_3, \kappa_5$  to 1 in the numerical computations.

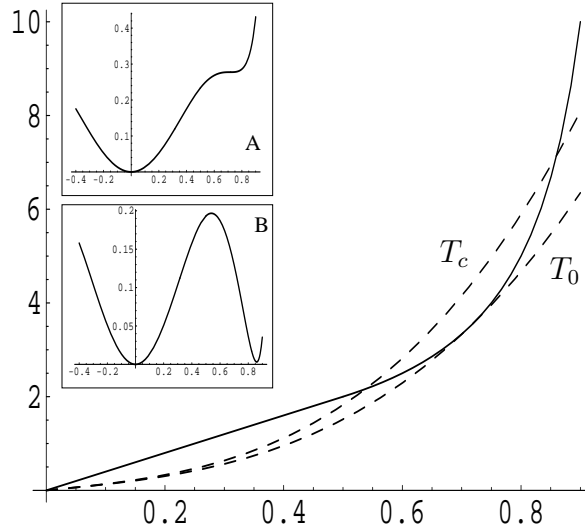


Figure 8: The main figure is the plot of left (dashed lines) and the right hand side (solid line) of the saddle point equations.  $T_0$  is the point where the two roots of (46) merge.  $T_c$  is the curve corresponding to the Hawking-Page transition temperature. The inserts A and B are the potentials corresponding to these temperatures

where the  $I_{1,2}$  are the action for the large and small black-holes respectively and  $\rho_{1,2}$  are the corresponding solutions in the matrix model. The constant  $f = \log(2) - 1/2$  is added to make the potential from (46) continuous at  $\rho = 1/2$ . Since the values of  $\rho_{1,2}$  are those at the extremum of the left hand side of (47), we have two more equations that are given by (46).

For a given temperature,  $T$ ,  $I_{1,2}$  are known from the gravity side, so the problem now is to solve the above equations for  $a(T)$ ,  $b(T)$  and  $\rho_{1,2}$ . We do this numerically. The solutions are plotted in Figure (7). Note that  $a(T)$  and  $b(T)$  increases monotonically. As a consequence of this the dashed line in Figure (8) that represents the left hand side of (46) moves towards  $T_c$  as the temperature is increased thus generating two solutions for  $\rho$  corresponding to the small and the big black holes in between.  $\rho = 0$  corresponding to the thermal  $AdS_5$  is always a solution.

Having known the variations of  $a(T, 0)$  and  $b(T, 0)$  with respect to the temperature we now incorporate the  $\alpha'$  corrections to  $I_{1,2}$  to get the first order dependence on  $1/\sqrt{\lambda}$ . We have

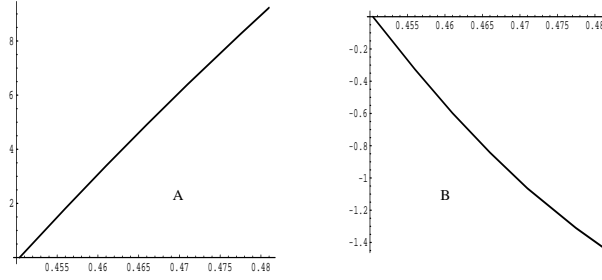


Figure 9: Plots of (A)  $\partial a(T)/\partial(1/\sqrt{\lambda})$  and (B)  $\partial b(T)/\partial(1/\sqrt{\lambda})$

$$\begin{aligned}
 a(T, 1/\sqrt{\lambda}) &= a(T, 0) + \frac{1}{\sqrt{\lambda}} \frac{\partial a(T)}{\partial(1/\sqrt{\lambda})} \Big|_{1/\sqrt{\lambda}=0} + \mathcal{O}(1/\lambda^{3/2}), \\
 b(T, 1/\sqrt{\lambda}) &= b(T, 0) + \frac{1}{\sqrt{\lambda}} \frac{\partial b(T)}{\partial(1/\sqrt{\lambda})} \Big|_{1/\sqrt{\lambda}=0} + \mathcal{O}(1/\lambda^{3/2}).
 \end{aligned}
 \tag{48}$$

The first order variations of equation (47) with respect to  $1/\sqrt{\lambda}$  gives,

$$2 \frac{\partial a(T)}{\partial(1/\sqrt{\lambda})} \rho_{1,2}^2 + 2 \frac{\partial b(T)}{\partial(1/\sqrt{\lambda})} \rho_{1,2}^4 = -\sqrt{\lambda} \delta I_{1,2}(T).
 \tag{49}$$

In the above equations,  $\delta I_{1,2}(T)$  are given by,

$$\begin{aligned}
 \delta I_{1,2}(T) &= \alpha' \beta (\delta F_{1,2}) \\
 &= -\frac{\beta}{\sqrt{2\lambda}} (3r_{1,2}^4 + 24r_{1,2}^2 + 9).
 \end{aligned}
 \tag{50}$$

From these we get the values of  $\frac{\partial a(T)}{\partial(1/\sqrt{\lambda})}$  and  $\frac{\partial b(T)}{\partial(1/\sqrt{\lambda})}$  shown in Figure (9).

The above analysis shows that the behavior of the coefficients as functions of temperature and  $\lambda$  are indeed the ones that we expect from the phases of the bulk theory as long as we concentrate on the black hole solutions with  $r_+ > \alpha'$ . The expansions are carried out about  $\lambda \rightarrow \infty$  as it was argued in [16] that the effective theory that is computed in the weak coupling falls in the same universality class as the one in the strong coupling limit. The addition of higher derivative term in the bulk does give information about  $1/\sqrt{\lambda}$  corrections, however this  $(a, b)$  model is unable to capture the phases including the smallest black hole solution. In the following section we will analyse this issue, in detail, by proposing another model which qualitatively reproduces various bulk phases of section 3.

## 6 A modified Matrix model

In this section we propose a modified (toy) matrix model which incorporate some of the additional qualitative features on the gravity side arised due to the GB term. We find, the minimal action that would reproduce these features need to be quartic in  $\rho^2$  and can be given by

$$S(\rho^2) = 2[A_4\rho^8 - A_3\rho^6 + A_2\rho^4 + (\frac{1-2A_1}{2})\rho^2] \quad , \quad (51)$$

where  $A_i$ 's are the parameters, which depend on the temperature as well as on the coupling constant. In the limit where the  $A_4$  and  $A_3$  vanish we get the  $(a, b)$  model [16].

The equations of motion ensuing from the action in (51) are given as follows. We write

$$F(\rho) = \frac{\partial S(\rho^2)}{\partial \rho^2} = [8A_4\rho^6 - 6A_3\rho^4 + 4A_2\rho^2 + (1 - 2A_1)]. \quad (52)$$

Then the equations in two different regions are

$$\rho F(\rho) = \rho \quad , \quad 0 \leq \rho \leq \frac{1}{2}, \quad (53)$$

$$= \frac{1}{4(1-\rho)} \quad , \quad \frac{1}{2} \leq \rho \leq 1. \quad (54)$$

The potentials that follows from the above action is given by

$$V(\rho) = -A_4\rho^8 + A_3\rho^6 - A_2\rho^4 + A_1\rho^2 \quad , \quad 0 \leq \rho \leq \frac{1}{2} \quad , \quad (55)$$

$$= -A_4\rho^8 + A_3\rho^6 - A_2\rho^4 + A_1\rho^2 - \frac{1}{4} \log[2(1 - \rho)] + \frac{1}{8} \quad , \quad \frac{1}{2} \leq \rho \leq 1. \quad (56)$$

The fact that there are four parameters instead of two has made the analysis technically more involved than  $(a, b)$  model [16]. In what follows, we will restrict ourselves to fixed values of  $A_1$  and  $A_4$  and study the features with the variation of two other parameters. We have chosen the values to be  $A_1 = .025$  and  $A_4 = 2.083$ . We have given plot of the potential against  $\rho$  in Fig.10. In order to make the extrema explicit we choose different scales for the potential for two different ranges of  $\rho$ , namely,  $0 \leq \rho \leq 0.5$  and  $0.5 \leq \rho \leq 1$ . The values of  $A_2$  and  $A_3$  are decreasing from the curve in bottom to that in top in the left figure of Fig.10 and from the curve on top to that in bottom in the right figure of Fig.10. There is always one minimum at  $\rho = 0$  where the potential vanishes.

Before we describe the variation of the potential with parameters a couple of comments are in order. The potential is not very sensitive to variation of  $A_4$  as it involves  $\rho^8$ . However, the potential is sensitive to variation of  $A_1$ . We have chosen

this particular value where it reproduces the features on the gravity side for  $\bar{\alpha} \leq \bar{\alpha}_c$  where one gets two minima. If we increase  $A_1$  the minimum in the  $\rho \leq .5$  approaches the one in  $\rho \geq .5$  and merges with it. Beyond that we get only one minimum which agrees with the feature on the gravity side for  $\bar{\alpha} \geq \bar{\alpha}_c$ . Finally as we will see in Fig.11 we need to choose values of  $A_2$  and  $A_3$  restricted within a particular region outside which the solution associated with the small black hole will have energy lower than the thermal AdS which we do not see on the gravity side. In the following, we give  $V(\rho)$  vs.  $\rho$  plots for different values of  $A_2$  and  $A_3$ :

- $(A_2, A_3) = (.45, 2)$ : There is one local minimum in the range  $\rho \leq 0.5$  and no extrema at  $\rho \geq 0.5$ . This corresponds to low temperature behaviour of GB black hole where we get only one small black hole solution.
- $(A_2, A_3) = (.4, 2)$ : A local maximum and a local minimum appear in the range  $\rho \geq 0.5$ . We identify this phenomenon with the nucleation of the big black hole and intermediate unstable black hole in the gravity picture.
- $(A_2, A_3) = (.385, 1.9375)$ : For further decrease of the parameters, the heights of the local minima increases and decreases in  $0 \geq \rho \geq 0.5$  and  $0.5 \geq \rho \geq 1$  respectively (Fig. 10) At this value of the parameters these two heights become equal. We can identify this point with a transition from small black hole to big black hole on the gravity side which is termed as HP1 transition.
- $(A_2, A_3) = (.38485, 1.93688)$ : (Due to close proximity this plot appears on the top of the earlier plot and not distinguishable for the present scale.) The height of the minimum in the range  $\rho \geq 0.5$  becomes zero and thus equal to the potential at  $\rho = 0$ . On the gravity side this corresponds to energy of big black hole reaching zero and becoming equal to that of thermal AdS triggering HP2 transition.
- $(A_2, A_3) = (.25, 1.5)$ : The height of the minimum in  $\rho \geq 0.5$  keeps on decreasing while in the region  $\rho \leq 0.5$  the local minimum becomes flat. This corresponds to the point beyond which the small black hole on the gravity side disappears.
- $(A_2, A_3) = (.248, 1.25)$ : As we decrease  $A_2$  and  $A_3$  further, the minimum in the left figure of Fig.10 ceases to exist while the minimum in the right figure of Fig. 10 becomes more and more deeper, in keeping with the fact that, at high temperature on the gravity side the only stable configuration remains is the big black hole.

As we see from the above analysis the coefficients decrease with temperature, unlike the behaviour of the coefficients in the  $(a, b)$ -model. This can be interpreted as the temperature gradient of the coefficients at the first order of inverse 't Hooft coupling has a negative sign relative to that at the zeroeth order. At this range, where appreciable  $1/\Lambda$  correction is taken into account, the contribution at first order dominates over that at zeroeth order.

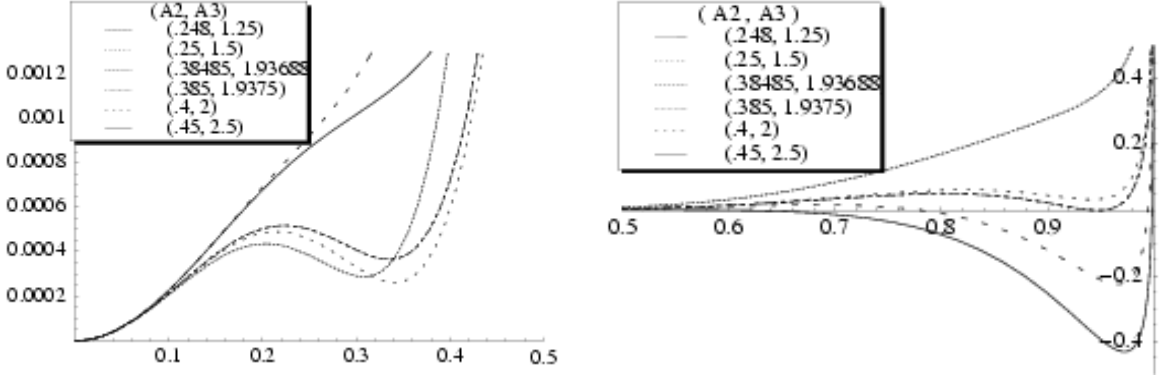


Figure 10: Potential as function of  $\rho$  for the range  $0 \leq \rho \leq 1/2$  (on left) and for the range  $0.5 \leq \rho \leq 1$  on right for increasing values of  $A_2$  and  $A_3$ . The different values of  $(A_2, A_3)$  are given above. The plots associated with  $(.38485, 1.93688)$  and  $(.385, 1.9375)$  are not distinct in this scale.

In order to analyse the saddle points, we consider the parametric plot of different critical points in the  $A_2$ - $A_3$  plane in Fig.11 keeping  $A_1$  and  $A_4$  fixed. As we vary the parameters we encounter a curve IV in the  $A_2$ - $A_3$  plane above which the saddle point associated with the small black hole has energy negative. From the analysis of black holes on the gravity side, it follows that the small black hole energy is always greater than thermal AdS ensuring the stability of the latter. So, in what follows, we restrict ourselves to the region below curve IV.

In the region bounded by IV, III and I, there are three saddle points. One is  $\rho = 0$  which corresponds to the thermal AdS. There are two more saddle points: a local maximum at  $\rho = \rho_-$  and a local minimum  $\rho = \rho_+$ . The latter corresponds to the small black hole that we obtain on the gravity side. There is no solution analogous to  $\rho_+$  in the gravity side. In the region bounded by II, III, IV and I, there appears two more saddle points. One of them  $\rho = \rho_1$  is a local maximum and the other one  $\rho = \rho_2$  is a local minimum. They correspond to the unstable, intermediate, and the stable big black hole respectively. In the region on the left hand side of curve I, the saddle points  $\rho = \rho_{\pm}$  cease to exist. In the region above the curve IV, as we have already

mentioned, the potential of the saddle point  $\rho = \rho_-$  becomes negative showing the energy of the associated small black hole on the gravity side becomes less than that of thermal AdS.

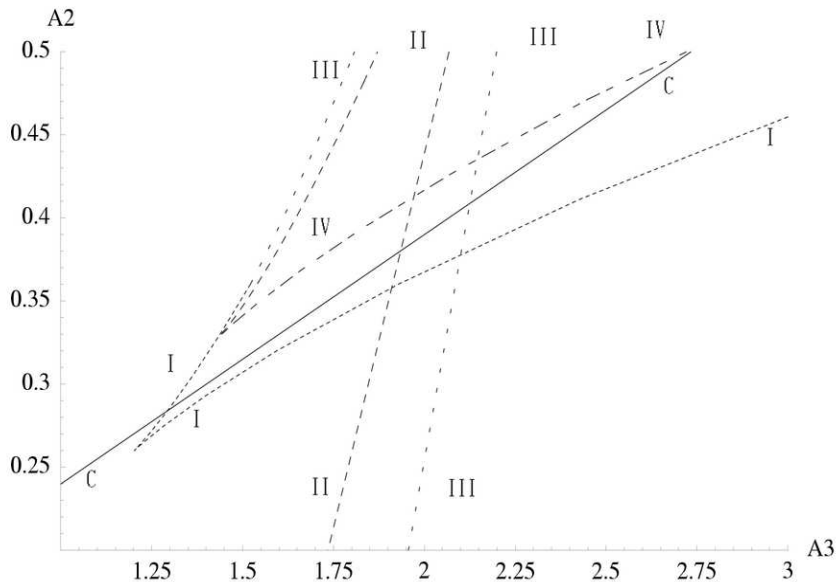


Figure 11: Parametric plots of different critical points in the  $A_2$ - $A_3$  plane. We choose  $A_1 = 0.25$  and  $A_4 = 2.083$ . In the region which is below or on the left side of curve I the saddle points  $\rho_{\pm}$  cease to exist. In the region above curve IV the potential of  $\rho_+$  vanishes. Curve II corresponds to HP transition and on curve III the saddle points  $\rho_1, \rho_2$  merge.

Similarly, the thermal history can be obtained from Fig.11 as follows. As we mentioned earlier,  $A_2$  and  $A_3$  will decrease with temperature along the curve C. As we follow the curve C from right to left, we find the  $\rho = 0, \rho_{\pm}$  are the solutions on the right of curve III. As we cross curve III, we encounter two additional saddle points  $\rho = \rho_1, \rho_2$ . Crossing the curve II corresponds to the Hawking-Page transition. As we cross curve I, the saddle point corresponds to the small black hole disappears.

As we see in the region on the bounded by the curve I, along with a local minimum ( at  $\rho = \rho_+$ ) we always obtain a local maximum ( at  $\rho = \rho_-$  ). This shows there is a bounce solution through which the tiny black hole decays. It will be interesting to understand this instability on the gravity side.

## 7 Discussion

In this paper, we have discussed phase transition of asymptotically AdS black hole solutions in presence of Gauss-Bonnet term. As long as  $\bar{\alpha}$ , strength of the coupling to GB term remains above certain critical value  $\bar{\alpha}_c$ , one gets a single black hole phase at any temperature. However, as the coupling comes down below the critical value two additional black holes appear. We called them small and intermediate black holes. The intermediate black hole is found to have negative specific heat. It turns out that this small stable black hole is a local minimum below a critical temperature. Beyond this temperature small black hole disappears. We have studied the associated phase diagram and find that the phase structure resembles that of van der Waals gas. In addition to the standard Hawking-Page transition, we have identified one more phase transition where the two branches of the phase diagram meet. We find the specific heat diverges at this new critical point.

From a different perspective, the Euclidean version of the black hole solution has been interpreted as the bounce mediating the decay of AdS orbifold into the bubbles of nothing. It was found earlier that for the radius of circle above a critical value the AdS orbifold is stable while below that bound the AdS orbifold decays. After adding the higher derivative terms in the action, we find that there is a bubble solution that exists for all values of the radius and has an energy density lower than that of AdS orbifold. This suggests that the AdS orbifold is unstable for any radius. One of the stringy features that we have addressed in this paper is the modification of decay rate in presence of a background string wrapped on the circle and we find the decay rate gets enhanced. It would be interesting to find tachyonic decay ensuing from wrapped black brane in this set up.

Five dimensional theory of gravity usually corresponds to some gauge theory on the boundary and the analysis on the gravity side has natural implications about the gauge theory. In absence of Gauss-Bonnet term, the gravity theory on Euclidean AdS (along with  $S^5$ ) is known to be dual to be pure N=4 SYM on a three sphere at finite temperature and the phase diagram associated with the gravity theory captures thermal history of N=4 SYM on  $S^3$ . In a similar spirit, we expect, dual of this five dimensional gravity theory in presence of Gauss-Bonnet term is some deformation of the above gauge theory and the phase diagram captures its thermal history. In [16], qualitative features of  $N = 4$  SYM on  $S^3$  was studied from the perspective of a matrix model. This model is phenomenological in nature and is characterised by two parameters  $(a, b)$ . On generic ground, one expects these parameters to be  $\lambda$  and  $T$

dependent. Appealing to the universal nature of this model near the critical points, we find out  $\lambda$  dependence of  $(a, b)$ . This is done by mapping the bulk  $\alpha'$  correction to the boundary. This method can easily be used to find similar  $1/\lambda$  dependence of matrix model coefficients in the case of other higher derivative corrections of the gravity action, such as,  $R^4$  term in IIB theory.

We have also proposed a modified matrix model that captures the qualitative features of the phase diagram of the bulk theory. Unlike  $(a, b)$  matrix model this model is non-universal and the phase diagram is reproduced only in a selected region of the parameter space. In addition the temperature dependence of the coefficients turn out to be different from usual linear increasing function. We also find there is a bounce through which the small black hole can decay. It will be interesting to identify this instability on the gravity side. We hope to return with some of these issues in future.

**Acknowledgements:**

We have benefited from discussions with Nabyendu Das, JianXin Lu, Balram Rai, Shibaji Roy, Gautam Tripathi and Spenta Wadia.

## References

- [1] S. Hawking and D. Page, Commun. Math. Phys. 87, (1983) 577.
- [2] J. M. Maldacena, Adv. Theor. Math. Phys. **2**, 231 (1998) [Int. J. Theor. Phys. **38**, 1113 (1999)] [arXiv:hep-th/9711200].
- [3] E. Witten, “Anti-de Sitter space, thermal phase transition, and confinement in gauge Adv. Theor. Math. Phys. **2**, 505 (1998) [arXiv:hep-th/9803131].
- [4] D. Birmingham, M. Rinaldi, Phys. Lett. b544 (2002) 316.
- [5] V. Balasubramanian and S. Ross, Phys. Rev. D66, (2002) 086002, hep-th/0205290.
- [6] E. Witten, Nucl. Phys. B195 (1982) 481.
- [7] E. Witten, Adv. Theor. Math. Phys. **2**, 253 (1998) [arXiv:hep-th/9802150].
- [8] M. Banados, Phys. Rev. D57, (1998) 1068, gr-qc/9703040.
- [9] M. Banados, A. Gomberoff and C. Martinez, Class. Quant. Grav. 15 (1998) 3757, hep-th/9805087.
- [10] S. Ross and G. Titchener, JHEP 0502 (2005) 021, hep-th/0411128.
- [11] V. Balasubramanian, K. Larjo and J. Simon, Class. Quant. Grav. 22 (2005) 4149, hep-th/0502111.
- [12] S. Kalyana Rama and B. Sathiapalan, Mod. Phys. Lett. A13 (1998) 3137, hep-th/9810069.
- [13] B. Sundborg, Nucl. Phys. B573 (2000) 349, hep-th/9908001.
- [14] O. Aharony, J. Marsano, S. Minwalla, K. Papadodimas and M. Van Raamsdonk, Adv. Theor. Math. Phys. 8 (2004) 603, hep-th/0310285.
- [15] H. Liu, *Fine structure of Hagedron transitions*, hep-th/0408001.
- [16] L. Alvarez-Gaume, C. Gomez, H. Liu and S. Wadia, Phys. Rev. D71 (2005) 124023, hep-th/0502227.
- [17] D. Boulware and S. Deser, Phys. Rev. Lett. 55 (1985) 2656.

- [18] T.K. Dey, S. Mukherji, S. Mukhopadhyay and S. Sarkar, to appear.
- [19] G. Horowitz, JHEP 0508 (2005) 091, hep-th/0506166.
- [20] R-G. Cai, Phys. Lett. B544, (2002) 176, hep-th/0206223.
- [21] M. Perry, "Instabilities in gravity and supergravity", In *Superspace and supergravity: Proceedings of the Nuffield Workshop*, Cambridge University Press, 1981.
- [22] K. Selivanov and T. Tomaras, JHEP 0210 (2002) 065, hep-th/0207172.
- [23] R. Myers, Nucl. Phys. B289 (1987) 701.
- [24] R-G. Cai, Phys. Rev. D65 (2002) 084014, hep-th/0109133.
- [25] M. Cvetič, S. Nojiri and S.D. Odintsov, Nucl. Phys. B628 (2002) 295.
- [26] Y. Cho and I. Neupane, Phys. Rev. D66 (2002) 024044, hep-th/0202140.
- [27] T. Torii and H. Maeda, Phys. Rev. D71 (2005) 124002, hep-th/0504127.
- [28] L. Cappiello and W. Muck, Phys. Lett. B522 (2001) 425, hep-th/0107238.
- [29] A. Biswas and S. Mukherji, Phys. Lett. B578 (2004) 425, hep-th/0310238.
- [30] S. Gubser, I. Klebanov and A. Tseytlin, Nucl. Phys. B534 (1998) 202, hep-th/9805156.
- [31] Y. Gao and M. Li, Nucl. Phys. B551 (1999) 229, hep-th/9811019.
- [32] K. Landsteiner, Mod. Phys. Lett. A14 (1999) 379, hep-th/9901143.
- [33] M. Caldarelli and D. Klemm, Nucl. Phys. B555 (1999) 157, hep-th/9903078.
- [34] A. Chamblin, R. Emparan, C. Johnson, R. Myers, Phys. Rev. D60 (1999) 064018, hep-th/9902170.
- [35] A. Chamblin, R. Emparan, C. Johnson, R. Myers, Phys. Rev. D60 (1999) 104026, hep-th/9904197.
- [36] A. Petrov, Class.Quant.Grav. 22 (2005) L83, gr-qc/0504058.
- [37] O. Aharony, J. Marsano, S. Minwalla, K. Papadodimas and M. Van Raamsdonk, Phys. Rev. D **71** (2005) 125018, hep-th/0502149.

- [38] P. Basu and S. R. Wadia, Phys. Rev. D **73** (2006) 045022, hep-th/0506203.
- [39] L. Alvarez-Gaume, P. Basu, M. Marino and S. R. Wadia, hep-th/0605041.